Supplementary Materials for
Universal conductance fluctuations and phase-coherent transport in a semiconductor Bi_2O_2Se nanoplate with strong spin-orbit interaction

Mengmeng Meng, [1] Shaoyun Huang, [1, *] Congwei Tan, [2, 3] Jinxiong Wu, [2]
Xiaobo Li,[1, 3] Hailin Peng[2, *] and H. Q. Xu[1, 4, 5, *]

[1]*Beijing Key Laboratory of Quantum Devices, Key Laboratory for the Physics and Chemistry of Nanodevices and Department of Electronics, Peking University, Beijing 100871, China*

[2]*Center for Nanochemistry, Beijing National Laboratory for Molecular Sciences (BNLMS), College of Chemistry and Molecular Engineering, Peking University, Beijing 100871, China.*

[3]*Academy for Advanced Interdisciplinary Studies, Peking University, Beijing 100871, China*

[4]*Beijing Academy of Quantum Information Sciences, West Bld. #3, No.10 Xibeiwang East Rd., Haidian District, Beijing 100193, China*

[5]*NanoLund and Division of Solid State Physics, Lund University, Box 118, S-221 00 Lund, Sweden*

[*] Corresponding authors: Professor H. Q. Xu (hqxu@pku.edu.cn), Dr. Shaoyun Huang (syhuang@pku.edu.cn) and Professor Hailin Peng (hlpeng@pku.edu.cn)

Contents

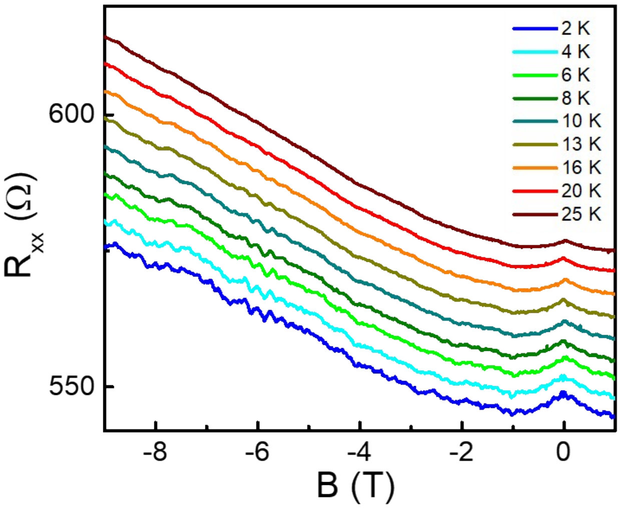

Figure S1. Measured longitudinal resistance (R_{xx}) of the same device as in the main article as a function of vertically applied magnetic field at temperatures of 2 to 25 K. For clarity, all the curves except for the one at 2 K are successively vertically offset. Here, the longitudinal resistance is obtained from $R_{xx} = V_x/I$ using lock-in technique [cf. the measurement circuit setup shown in the inset of Fig. 2(b) in the main article]. As we sweep the field, similar conductance fluctuations superposed on top of the background magnetoresistance are observable at different temperatures. The zoom-in plots in the vicinity of zero field show WAL characteristics at low temperatures and a WAL-WL crossover as temperature increases (cf. the results shown in the main article).

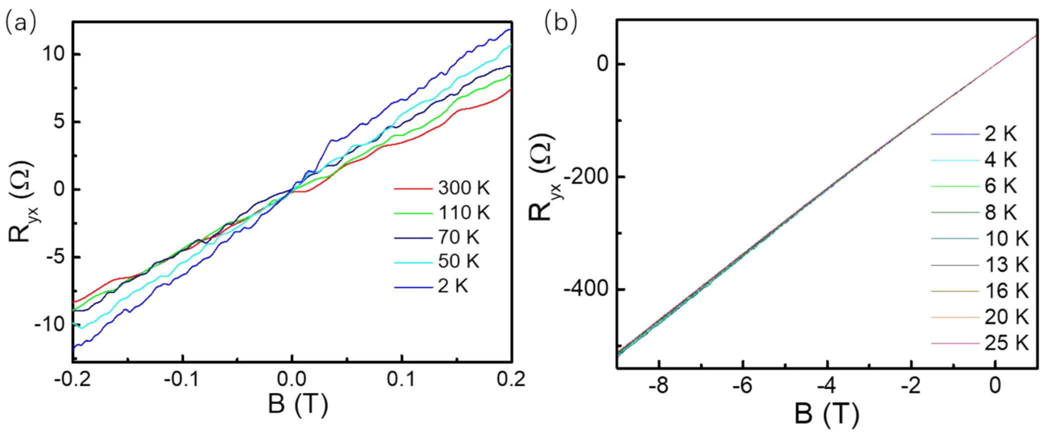

Figure S2. Transverse resistance (R_{yx}) of the device vs. vertically applied magnetic field B at different temperatures. As the schematic shown in the inset of Fig. 2(b) in the main article, we measure V_x and V_y simultaneously using lock-in technique and the Hall resistance is obtained by $R_{yx} = V_y/I$. (a) R_{yx} in a small, low-field region and (b) R_{yx} over a large region of fields. The sheet carrier density n_{sheet} is determined from the low-field Hall coefficient as $R_H = 1/ne$ with the Hall coefficient determined by the slope of $R_H = R_{yx}/B$.

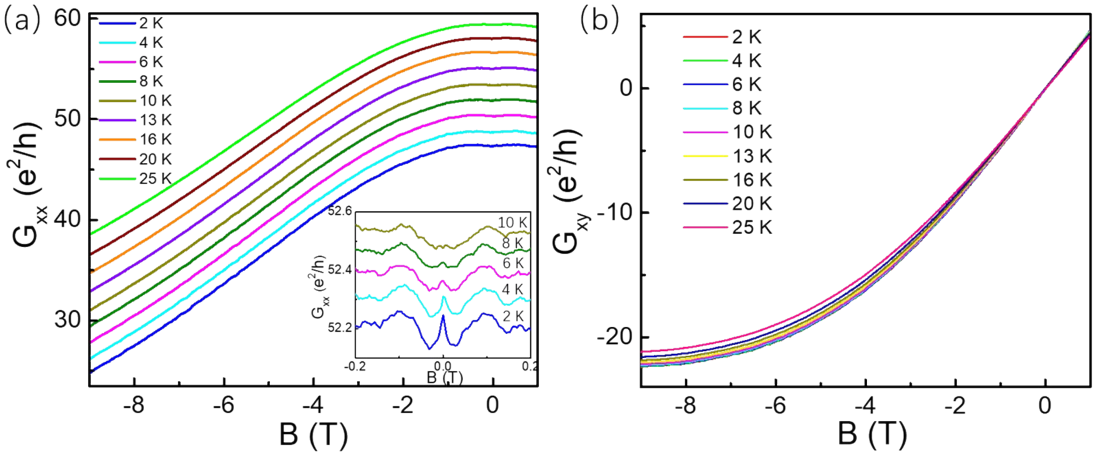

Figure S3. (a) Longitudinal conductance G_{xx} of the device vs. vertically applied magnetic field B at different temperatures. (b) Transverse conductance G_{xy} of the device vs. vertically applied magnetic field B at different temperatures. Here G_{xx} and G_{xy} can be calculated from measured R_{xx} and R_{yx} as $G_{xx} = \frac{R_{xx}}{R_{xx}^2 + R_{yx}^2}$ and $G_{xy} = \frac{R_{yx}}{R_{xx}^2 + R_{yx}^2}$. Longitudinal conductance fluctuations δG shown in Fig. 4(a) in the main article are obtained by subtracting the polynomial backgrounds from the measured dada shown in (a). The inset in (a) shows zoom-in plots of the conductance around zero field. For clarity, all the curves in (a) except for the one at 2 K are successively vertically offset.

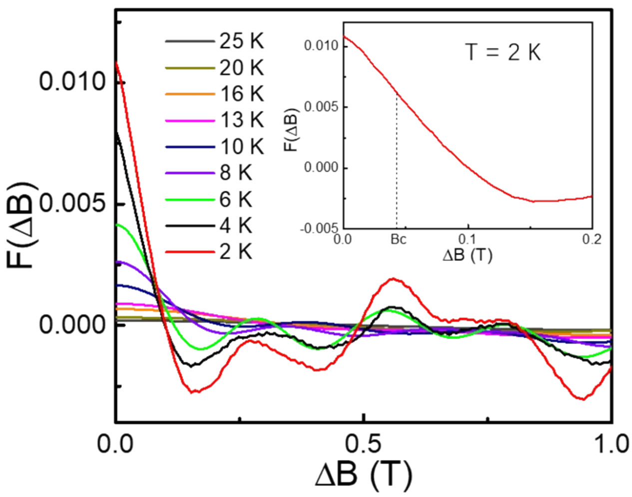

Figure S4. Autocorrelation function F(ΔB) of the measured conductance fluctuations shown in Fig. 4(a) in the main article. The characteristic field B_c obtained at the half maximum $F(B_c) = \frac{1}{2}F(0)$ in each plot is related to phase coherence length L_φ by

$\Phi_0 = L_\varphi^2 B_c$, where Φ_0 is the flux quantum. The inset shows a zoom-in plot of F(ΔB) at 2K, demonstrating how B_c is determined from F(ΔB). The extracted values of L_φ from the autocorrelation functions at different temperatures are shown in Fig. 4(c) in the main article.

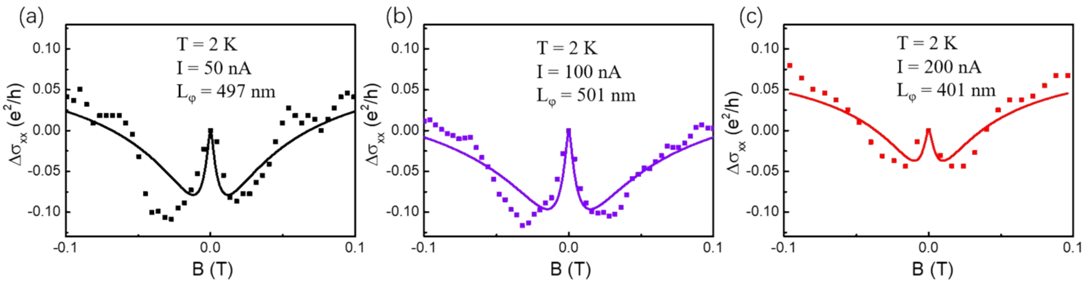

Figure S5. Magnetoconductivity of the same device as in the main article measured at 2 K with an excited current of (a) 50 nA, (b) 100 nA (the same as in Fig. 3c of the main article), and (c) 200 nA. Dots are measurement data and solid lines are the results of best fits of the measurement data to Eq. (1) of the main article. It is found that the extracted phase coherence length L_φ of carriers from the measurements with an excited current of 100 nA is almost the same as that extracted from the measurements with a 50 nA excitation current, but is much larger than the value extracted from the measurements with a 200 nA excitation current. Thus, the effect of bias current heating on the phase coherent length in the device is negligible in the temperature range considered in the main article.